

# Plasma Nitriding Behavior of DIN 1.2344 Hot Work Tool Steel

S. Karimzadeh<sup>1\*</sup>, F. Mahboubi<sup>2</sup> and G. Daviran<sup>2</sup>

\* Safoura.karimzadeh@gmail.com

Received: September 2019

Revised: June 2020

Accepted: August 2020

<sup>1</sup> Department of Materials Engineering, Faculty of Mechanical Engineering, University of Tabriz, Tabriz, Iran

<sup>2</sup> Department of Mining and Metallurgical Engineering, Amirkabir University of Technology, Tehran, Iran

DOI: 10.22068/ijmse.17.4.1

**Abstract:** In the present investigation the effect of time and temperature on plasma nitriding behavior of DIN 1.2344 (AISI H13) steel is studied. Pulsed plasma nitriding process with a gas mixture of  $N_2 = 25\% + H_2 = 75\%$  and duty cycle of 70% is applied to cylindrical samples of DIN 1.2344 hot worked tool steel. X-ray diffraction, surface roughness, microhardness and ball on disc wear tests are performed and the behavior of plasma nitrided samples are compared. Scanning electron microscopy and optical microscopy are used in order to observe the microstructure of samples after nitriding. XRD results showed that the compound layer consists of dual phase. Hardness near the surface dropped by rising the process temperature and it increased with longer process duration. The comparison of  $\mu$  results showed that, frictional properties at longer duration and lower temperature is similar to higher temperature and shorter duration.

**Keywords:** Plasma nitriding, Friction coefficient, Effects of parameters, DIN 1.2344 tool steel.

## 1. INTRODUCTION

DIN 1.2344 hot worked tool steel, an important and common steel, can be used as a die for forging, extrusion, other hot working applications and aluminum injection [1-4]. High ductility, good hardening ability and low dimensional changes during heating and cooling are the key features of this steel [5]. In hot forming operations, the surface of the mold is vulnerable; Wear and thermal fatigue mostly cause the molds failure that can be controlled by surface operations [1, 6]. Surface modification by plasma nitriding affects material properties such as wear, fatigue, corrosion resistance and improves steel resistance against them [7-9]. Plasma nitriding has advantages over other nitriding methods (salt bath nitriding and gas nitriding), because it is easier to control the process conditions to achieve optimal properties [8, 10]. Plasma nitriding is also carried out under the aging temperature of the steel and prevents over aging of the steel core [11]. Due to the interaction of nitrogen with steel elements, during the nitriding process, two different layers are formed on the steel surface. The first layer, from the top of the steel is named the compound layer which, usually consists of  $\epsilon$  ( $Fe_2-3N$ ) and  $\gamma'$  ( $Fe_4N$ ) iron nitrides. The second layer placed under the compound layer consists of dissolved nitrogen in the ferrite lattice and is called the diffusion layer [12, 13]. When the nitrogen

solubility in iron reaches its maximum limit, nitrides precipitate in the diffusion region and produce fine coherent precipitations [14]. The compound layer consists of either mixed  $\epsilon$  and  $\gamma'$  phases or a single-phase of  $\epsilon$  or  $\gamma'$ .

There are many parameters in plasma nitriding operation that impress wear and frictional properties [15-17]. Time of nitriding and process temperature are both significant parameters that change the resulting structure like the thickness of the compound and the diffusion layer. For this reason, wear properties are not similar for samples in different nitriding conditions. As shown in Fig. 1, ball on disc wear test is done for the plasma nitrided samples. When the ball and disc (sample) are in contact, a track is created by the ball on the surface of the disc.

Wear properties of AISI H13 tool steel (DIN 1.2344), such as weight loss and wear rate are investigated by previous researchers. The results showed that wear properties of the hot work AISI H13 tool steel vary when one parameter changes (i.e. temperature or time), depending on the thickness of the nitrided layer and the hardness [18, 19]. However, in all of these papers, there is no comparison between the effects of parameters on the plasma nitriding behavior.

The aim of this work is to study and compare effects of plasma nitriding parameters (time and temperature) on diverse properties such as

thickness of the nitrided layer, surface roughness, wear properties, etc. The operation time and temperature changed in 3 levels and conditions are given in Table 1. The thickness of the diffusion and compound layer, variations of friction coefficient and width of the wear scar have been compared for different conditions. Also, the effective diffusion coefficient of nitrogen and onset time in DIN 1.2344 steel are calculated.

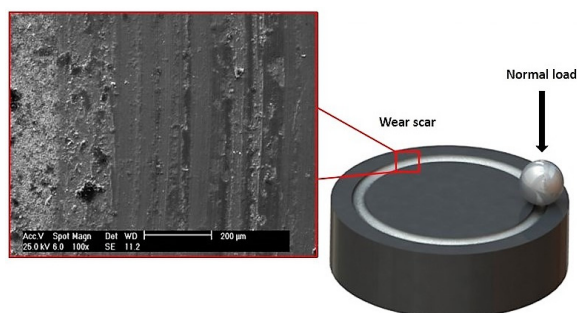


**Fig. 1.** Schematic illustration of ball on disc wear test and SEM image from the wear track

## 2. EXPERIMENTAL PROCEDURE

Cylindrical samples of DIN 1.2344 hot work tool steel were used in this study for plasma nitriding and subsequent tests. Before plasma nitriding, samples were heat treated °C to reach a mean hardness of 500 HV. Then, all samples were prepared according to the conventional metallographic techniques.

Pulsed plasma nitriding process was done in a gas mixture of 25 vol. % N<sub>2</sub> and 75 vol. % of H<sub>2</sub>, duty cycle of 70%, total pressure of 4 mbar and hot wall temperature of 420 °C for all specimens. The roughness of nitrided specimens and the untreated (Q&T) specimen all were measured by a Time Group TR 200 type roughness meter. Before the SEM tests, plasma nitrided samples were prepared in this way: First nitrided samples were sliced and mounted in Bakelite, polished with SiC abrasive paper, then mirror polished with Alumina suspension (1 μm) and cleaned in alcohol. The nitrided layers were

appeared by chemical etching with Nital 2%. The cross-section micrograph and the wear scar were analyzed using a Philips XL30 scanning electron microscopy. The phases were determined by X-ray diffraction analyzes using an Equinox diffractometer. Tribological tests of nitrided samples were evaluated using a ball on disc custom design tribotester. The ball was configured to contact the disc (nitrided sample) under a load of 10 N. The sliding distance was 1000 m for all samples. During the wear test, the coefficient of friction was calculated and displayed on the computer screen. All tests were conducted at room temperature without any lubricant. Microhardness was measured with Shimadzu microhardness tester with a Vickers indenter. Nitriding temperature and time were changed and different conditions are summarized in Table 1.

## 3. RESULTS AND DISCUSSION

Representative cross-sectional SEM and OM micrographs of samples S<sub>2</sub> and S<sub>5</sub> including the compound layer and the diffusion layer are shown in Fig. 2. Thickness values of these layers for different specimens are given in Table 1. Thickness of the diffusion and the compound layer depends upon nitriding time and temperature. In a fixed time of 8 hours, with an increase in the temperature from 520 °C up to 540 °C, the thickness of the diffusion layer increased from 108 μm to 155 μm. Moreover, the diffusion depth for sample S<sub>4</sub> changed to 142 μm by changing the temperature to 530 °C. Due to the Arrhenius's law ( $D = D_0 \exp(-Q/RT)$ , in which  $D$ ,  $D_0$ ,  $Q$ ,  $R$ , and  $T$  are the diffusion coefficient, the diffusion constant, the activation energy, the gas constant and the absolute temperature), the diffusion coefficient of nitrogen in steel depends on nitriding temperature. When the temperature increases, the penetration depth of nitrogen increases too. Additionally, the thickness of the diffusion layer

**Table 1.** Plasma nitriding conditions, structural and wear properties, for nitrided samples.

| sample         | Time (h) | Temperature (°C) | Compound layer (μm) | Diffusion layer (μm) | Coefficient of friction or $\mu$ | Width of scar (μm) |
|----------------|----------|------------------|---------------------|----------------------|----------------------------------|--------------------|
| S <sub>1</sub> | 6        | 520              | 4                   | 99                   | 0.44                             | 815                |
| S <sub>2</sub> | 16       | 520              | 7                   | 192                  | 0.35                             | 473                |
| S <sub>3</sub> | 8        | 520              | 4.5                 | 108                  | 0.37                             | 766                |
| S <sub>4</sub> | 8        | 530              | 7.5                 | 142                  | 0.36                             | 728                |
| S <sub>5</sub> | 8        | 540              | 9                   | 155                  | 0.35                             | 707                |

grows from 99 to 108 and then 192  $\mu\text{m}$  as a result of nitriding time addition from 6 to 8 and 16 hours at a constant temperature of 520  $^{\circ}\text{C}$  (samples  $S_1$ ,  $S_3$ ,  $S_2$ ). Since the diffusion process depends on time, longer operation time gives nitrogen atoms this opportunity to penetrate into the depth of the work piece. the relative diffusion depths are comparable with double and triple gas nitrided H13 steel, 135 and 180  $\mu\text{m}$ , respectively available in the literature [20]. Jacobsen [8] and coworkers reported 40-80  $\mu\text{m}$  diffusion layer thickness in low temperature and low current density plasma nitriding. The thickness of the compound layer grows up gradually by increasing time and temperature (Table 1). As the temperature rises slightly by 20  $^{\circ}\text{C}$ , the thickness of the compound layer doubles ( $S_3$  and  $S_5$ ). When the time of process reduplicates the thickness of the compound layer rises to one and a half times ( $S_3$  and  $S_2$ ). This shows; that low changes in the temperature have more effects on thickness of the white layer. In other words, the compound layer thickness depends more on the temperature than the time.

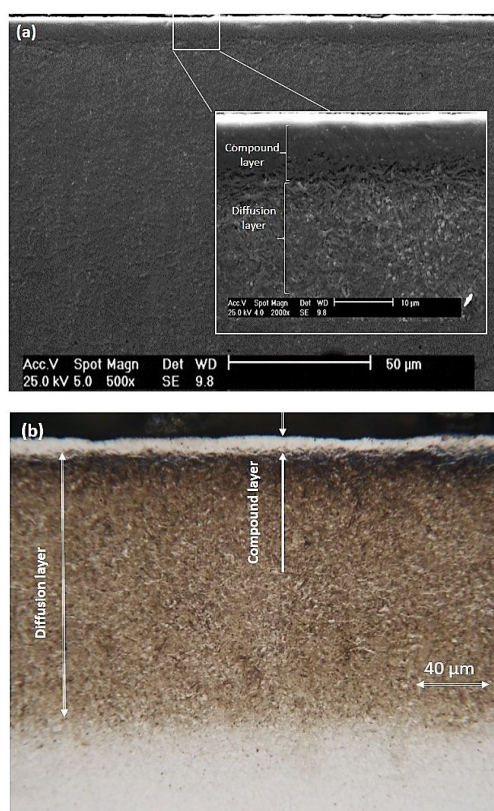


**Fig. 2.** Cross sectional SEM and OM micrographs of samples a)  $S_2$  and b)  $S_5$ .

With a reference to  $d = (D_e t)^{0.5} + C$  ( $t$  and  $D_e$  are time of nitriding and empirical effective diffusion coefficient) the empirical effective diffusion is a dependent parameter to in-diffusional and trapping of nitrogen. The equation constant ( $C$ ) is a term that represents onset time. The equation implies that there is a linear relationship between case depth ( $d$ ) and  $t^{0.5}$ . Experimental data for the penetration depth from Table 1 are plotted in Fig. 3. The figure corresponds to the above equation because there is a linear relationship between square root of the time and the penetration depth. The effective diffusion coefficient of nitrogen in the ferrite lattice and onset at 520  $^{\circ}\text{C}$  for DIN 1.2344 steel are calculated  $1.069 \times 10^{-12} \text{ m}^2/\text{s}$  and 0.95 h respectively. As already mentioned, the effective diffusion coefficient depends on the trapping of nitrogen by the alloying elements. Therefore, the more alloying elements, the less diffusion coefficient. Effective diffusion coefficient of nitrogen for AISI 4140 steel and stainless steel were calculated in the studies of Berg [14] and Corengia [21] and the values were reported  $3.18 \times 10^{-12} \text{ m}^2/\text{s}$  and  $0.4 \times 10^{-12} \text{ m}^2/\text{s}$ , respectively. AISI 4140 steel with a lower alloying element than AISI H13 (DIN 1.2344) tool steel has a larger effective diffusion coefficient and the stainless steel with more alloying elements than the H13 steel has a lower effective diffusion coefficient. The comparison shows the validity of the effective diffusion coefficient of DIN 1.2344 tool steel. Also, the penetration depth of nitrogen in DIN 1.2344 steel at 520  $^{\circ}\text{C}$  and gas composition of  $\text{N}_2 = 25\% + \text{H}_2 = 75\%$  after 25 hours is estimated (251  $\mu\text{m}$ ).

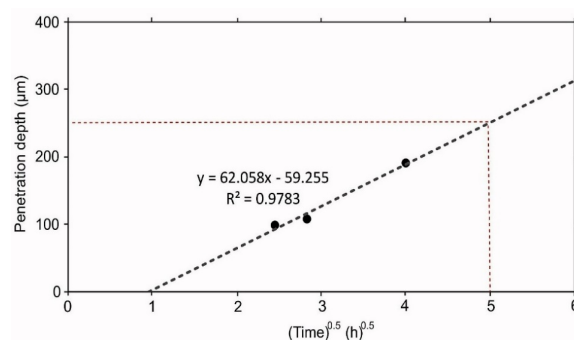


**Fig. 3.** The penetration depth versus square root of time for plasma nitrided DIN 1.2344 tool steel at 520  $^{\circ}\text{C}$ .

X-ray diffraction patterns for plasma nitrided samples in different conditions are shown in Fig. 4. The absence of iron peaks indicate that the nitrided layer is thick. The patterns illustrate that in all nitrided samples the compound layer is dual phase and it is made of mixture of  $\epsilon$  and  $\gamma'$  phases, but the intensity of diffraction peaks for these phases are different. While the amount of  $\gamma'$  phase increases by increasing the temperature, the intensity of diffraction peaks of the  $\epsilon$  phase goes down gradually. There are two reasons behind this behavior: 1) according to the Fe-N-C phase diagram, in low carbon contents, the compound layer accompanies by the formation of the  $\gamma'$  phase. At higher temperatures (here 540 °C) surface sputtering leads to decarburizing of the surface. Therefore, high sputtering speed is an effective factor in the formation of  $\gamma'$  phase [22, 23]. 2) As the nitriding temperature goes up, the diffusion rate of nitrogen atoms from the surface to the depth increases and the lack of replacement of the nitrogen ions from the plasma causes the formation of the  $\gamma'$  phase.

The comparison of  $S_1$  and  $S_2$  samples reveals that the amount of both  $\epsilon$  and  $\gamma'$  phases grow by increasing the time. In other words, the surface has enough opportunity to prepare more nitrides as a result of long durations. Many factors affect the formation of  $\epsilon$  and  $\gamma'$  iron nitrides, the most important are temperature and gas composition. Since the gas composition of all specimens is fixed to 25% nitrogen and 75% hydrogen, the temperature plays an important role in the formation of these two phases.  $\epsilon$  iron nitride is rich in nitrogen so it can be considered that  $\gamma'$  iron nitride forms before the  $\epsilon$  phase. When the nitrogen gas is sufficient, a layer of  $\gamma'$  iron nitride forms on the surface then,  $\epsilon$  phase forms on the top of the  $\gamma'$  layer and the compound layer become dual phase [24].

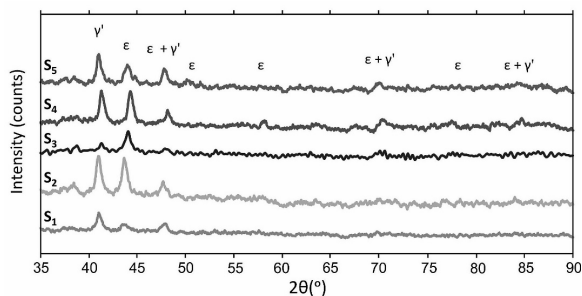


Fig. 4. XRD patterns for nitrided samples in different operation times and temperatures.

Fig. 5 illustrates the average surface roughness results ( $R_a$ ) for plasma nitrided samples. The measured roughness of the untreated sample (Q&T) was about 0.008  $\mu\text{m}$ . Surface roughness values for nitrided samples show that the nitride particles make the surface rougher and the surface roughness rises up after plasma nitriding. It is observed in Fig. 5(a) that the surface roughness is increased with the nitriding temperature leading to the 0.177  $\mu\text{m}$  in 540 °C ( $S_3$ ,  $S_4$ ,  $S_5$ ). Karamiş et al. [25] are in agreement with an increment of roughness from 1.3  $\mu\text{m}$  up to 2.8  $\mu\text{m}$  in 530 °C and 550 °C respectively. Fig. 6 shows a SEM image from the surface of samples. Nitride precipitates can be seen clearly in the image and as the temperature rises from 530 °C to 540 °C ( $S_4$  and  $S_5$ ), precipitates become coarser.

Fig. 5 (b) shows the effect of operation time on surface roughness ( $S_1$ ,  $S_2$  and  $S_3$ ). The roughness in 6 and 8 hours is approximately unchanged but in longer durations (here 16 hours), it drops to the minimum amount of 0.084. Das et al. [26] observed a rougher surface after duplex plasma nitriding for 6, 12 and 24 as well as the minimum  $R_a$  which was 0.35. In conclusion, the generated nitrided layer in this paper is more uniform.

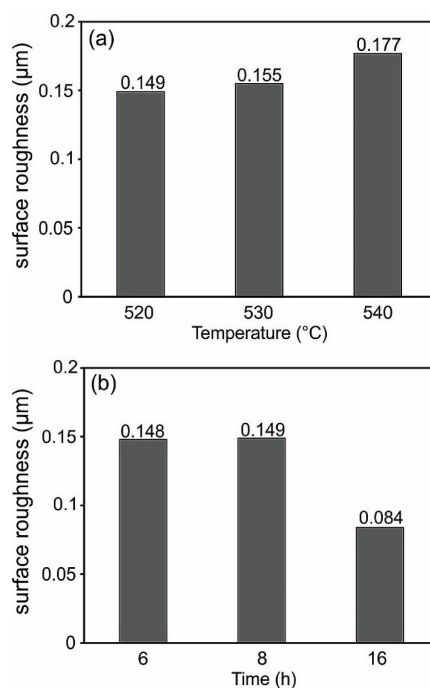


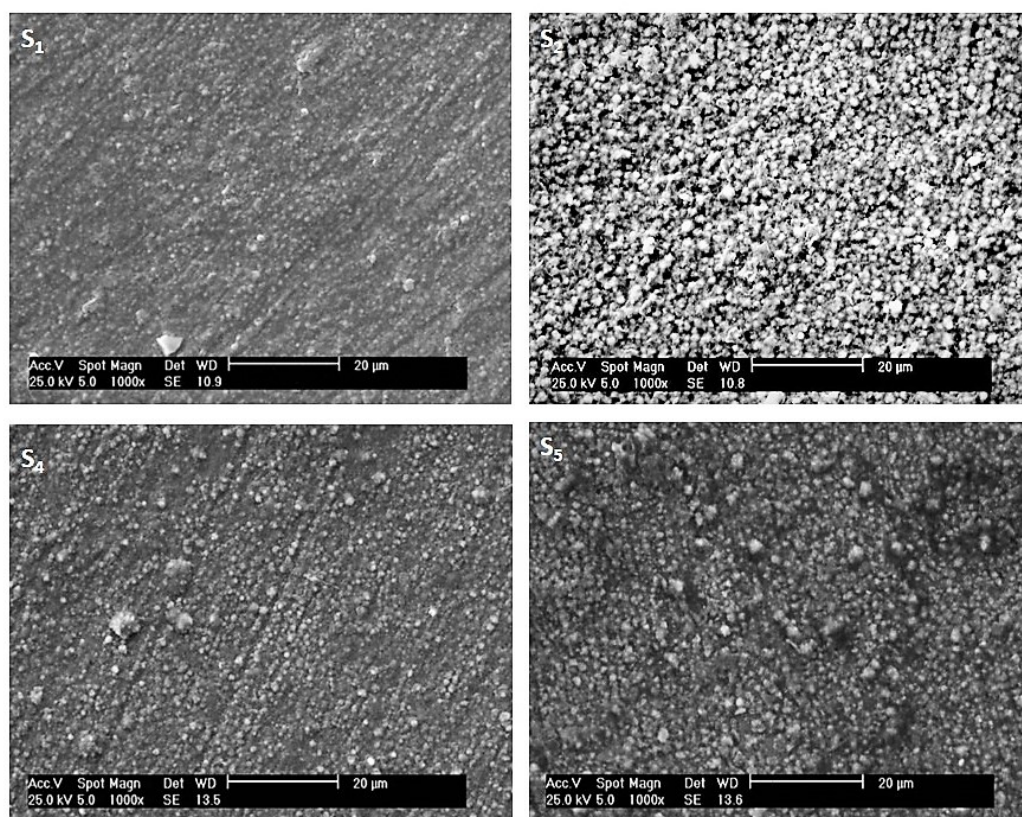
Fig. 5. Surface roughness as a function of nitriding a) temperature, b) time.

Fig. 6 reveals the coarsening of nitrides in sample  $S_2$  in comparison to  $S_1$ . Although, effects of deposits on the roughness is undeniable, it should be noted that there is an important phenomenon against increasing the surface roughness that is called sputtering and redeposition. In other words, during the plasma nitriding, numerous actions happen in opposite directions. While the nitrides deposit on the surface of the steel, particles are carried by the sputtering of the surface from the top sites to the spoiled areas and redeposit there. Hence, the surface roughness reduces in 16 hours.

Microhardness profiles of nitrided samples are given in Fig. 7. The test, started from the surface of specimens and continued until reaching the interface of the nitrided layer with the substrate and the substrate itself. The hardness increases gradually from the substrate to the surface in all samples and the maximum hardness near the surface is related to the sample  $S_2$ . The prolonging process from 6 to 16 hours causes the hardness near the surface to rise up from 860 HV to 1190 HV ( $S_1$  and  $S_2$ ). Moreover, hardness near

the surface for the same steel in 510 °C after plasma nitriding for 25 hours is reported 1250 HV by Karamiş [19].

When the operating temperature rises from 520 °C to 530 and then 540 °C, the hardness of the case depth increases due to the increase in the diffusion coefficient of nitrogen [27, 28]. But because of the reduction in the amount of  $\epsilon$  phase with HCP crystalline structure and increasing the amount of  $\gamma'$  phase with FCC crystalline structure (XRD results), hardness near the surface decreases. In plasma nitriding process, hardness of the surface increases with mechanisms such as interstitial solid solution of nitrogen atoms in iron lattice and formation of fine coherent precipitates in the matrix which avoid dislocation's movements. The profile slope at 520 °C ( $S_3$ ) is sharp and with the further increase of the nitriding temperature ( $S_4$  and  $S_5$ ), this slope decreases. The reason is at 520 °C (lowest temperature in this study), nitrogen atoms at the surface of the specimen could not penetrate enough into the core and accumulate at the surface then the hardness difference near the surface and the core increases.



**Fig. 6.** SEM image from the surface of samples after plasma nitriding.

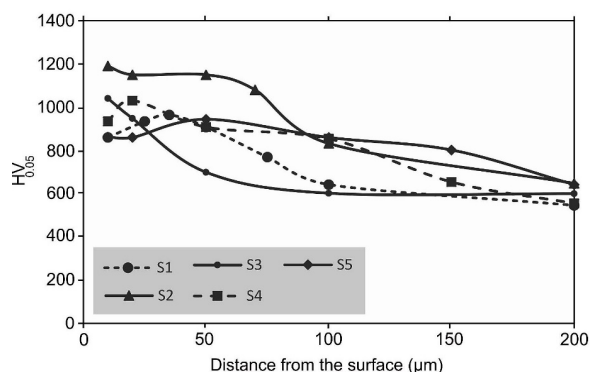


**Fig. 7.** Hardness- depth profile for plasma nitrided specimens under different conditions.

Fig. 8 shows the friction coefficient versus the distance curves obtained from the wear tests. The relevant friction coefficient for each condition is summarized in Table 1. All  $\mu$  results are in the range of 0.35 up to 0.37 except sample  $S_1$  that is 0.44. By considering samples  $S_3$ ,  $S_4$ ,  $S_5$  it seems the temperature doesn't have a significant effect on changing  $\mu$  values and it only differs by 0.01. Table 1 also shows that  $\mu$  reduces mildly by increasing nitriding time from 6 to 16 hours. The reason is that the magnitude of the friction coefficient is affected by the amount of  $\epsilon$  iron nitride because of its hexagonal close-packed structure, high hardness and non-metallic nature [11, 29]. Castro et al. [18] reported a mean value of  $\mu=0.5$  for salt- bath nitrided H13 steel. Wei et al. [30] obtained larger  $\mu$  (1.2) under the 50N load at room temperature and they mentioned in higher temperatures it reduces severely to 0.8.

The comparison of the  $\mu$  results illustrates that the friction coefficient of the sample  $S_2$  (nitrided for 16 hours at 520 °C) is equal to the friction coefficient of the sample  $S_5$  (nitrided at 540 °C for 8 hours). Simply put, with an increase of just 20 °C in temperature under completely equal conditions, the operating time can reduce for 8 hours to obtain the same friction coefficient. SEM micrograph of the scratched surface and the width of wear track are demonstrated in Fig. 9. It is shown the width of wear track varies in the diverse times and temperatures (Table 1). Sample  $S_2$  with a maximum hardness has shown the best resistance to wear and sample  $S_1$  maximum width of wear track among the others. Saklakoglu [31] was reported that under the 5N load the width of wear track for the H13 tool steel after Nitrogen ion implantation varies from 240 up to 320  $\mu\text{m}$ . Aydin et al. [32] observed 555  $\mu\text{m}$  mean width of

wear track after chromium coating under the load of 2N. The comparisons show plasma nitriding acts well under the 10N load. While, the white layer prevents the adhesion of the ball to the surface of the specimen and reduces the friction coefficient, it is a very brittle layer due to its high hardness. So, during the wear test not only it fractures to the abrasive particles and smaller components but also it rises the wear rate [33]. The diffusion layer underneath the white layer acts like a rigid substrate and prevents crushing of the surface to abrasive particles. The thickness of the diffusion layer for the sample  $S_2$  is approximately 1.2 times larger than the sample  $S_5$ . Thus, the sample  $S_2$  has a high resistance to the indenting and slipping of the ball than the sample  $S_5$ . Also, the width of wear track for the sample  $S_5$  is approximately 1.5 times larger than the sample of  $S_2$ . Therefore, the diffusion layer has a significant effect on reducing the width of the wear track. Although the friction coefficient of sample  $S_4$  is 0.36, the width of wear track is 728  $\mu\text{m}$  which shows the nitrided layer was not strong enough to resist the load of the ball.

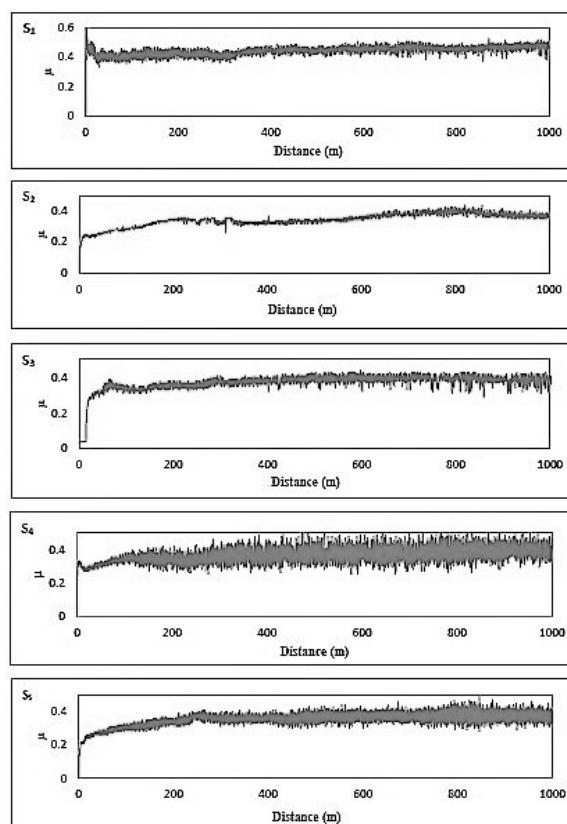


**Fig. 8.** The friction coefficient versus distance, for nitrided samples.

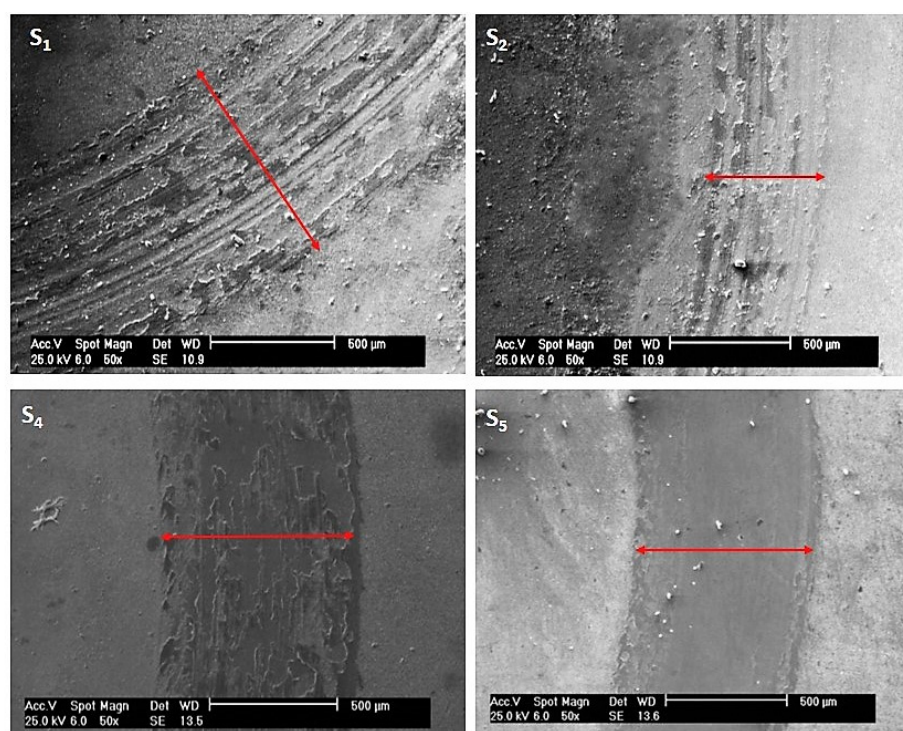


Fig. 9. SEM image of the wear groove and the width of track for plasma nitrided samples.

#### 4. CONCLUSION

The basic aim of this study was to compare the effect of time and temperature on plasma nitriding behavior of DIN 1.2344 hot worked tool steel. The temperature and time changed at 3 levels to see the behavior variations.

Thickness of the compound layer changed as a function of the temperature and the time. The thickness of this layer was more dependent on the temperature. A linear relationship was achieved between the penetration depth and square root of the time. The effective diffusion coefficient of nitrogen and onset time estimated at  $1.069 \times 10^{-12} \text{ m}^2/\text{s}$  and 0.95 h, respectively.

Surface roughness reduced by elapsing the time. This could be related to the Sputtering and redeposition of the surface in longer durations.

The compound layer was dual phase in all samples. The amount of  $\epsilon$  iron nitride decreased by increasing the temperature. Also, it increased by prolonging the time of nitriding.

Hardness near the surface was related to the amount of  $\epsilon$  iron nitride. By increasing the temperature, hardness near the surface reduced, whereas it increased when the time elapses. Higher hardness of the diffusion layer resulted to a lower width of wear track. The thicker diffusion layer, the narrow width of wear track.

#### ACKNOWLEDGMENT

The authors would like to thank Amirkabir University of Technology for financial supports. We also appreciate Omid Sharif Ahmadian and Tohid Pouraman for being helpful in laboratories.

#### REFERENCES

1. Wang, B., Zhao, X., Li, W., Qin, M. and Gu, J., "Effect of Nitrided-Layer Microstructure Control on Wear Behavior of AISI H13 Hot Work Die Steel." *Appl. Surf. Sci.*, 2017, 431, 39-43.
2. Leite, M. V., Figueroa, C. A., Gallo, S. C., Rovani, A. C., Basso, R. L. O., Mei, P. R., Baumvol, L. J. R. and Sinatora, A., "Wear Mechanisms and Microstructure of Pulsed Plasma Nitrided AISI H13 Tool Steel." *Wear*, 2010, 269, 466-472.
3. Birol, Y., "Analysis of Wear of a Gas Nitrided H13 Tool Steel Die in Aluminum Extrusion." *Eng. Fail. Anal.*, 2012, 26, 203-210.
4. Jacobsen, S. D., Hinrichs, R., Baumvol, I. J. R., Castellano, G. and Vasconcellos, M. A. Z., "Depth Distribution of Martensite in Plasma Nitrided AISI H13 Steel and its Correlation to Hardness." *Surf. Coat. Technol.*, 2015, 270, 266-271.

5. Taherkhani, K. and Mahboubi, F., "Investigation Nitride Layers and Properties Surfaces on Pulsed Plasma Nitrided Hot Working Steel AISI H13." *Iran. J. Mater. Sci. Eng.*, 2013, 10, 29-36.
6. Kumar, A., Kaur, M., Singh, S., Joseph, A., Jhala, G. and Bhandari, S., "High-Temperature Tribological Studies of Plasma-Nitrided Tool Steels." *Surf. Eng.*, 2018, 34, 620-633.
7. Karamiş, M. B., "Experimental Study of the Abrasive Wear Behaviour of Plasma-Nitrided Gearing Steel." *Wear*, 1993, 161, 199-206.
8. Jacobsen, S. D., Hinrichs, R., Aguzzoli, C., Figueroa, C. A., Baumvol, I. J. R. and Vasconcellos, M. A. Z., "Influence of Current Density on Phase formation and Tribological Behavior of Plasma Nitrided AISI H13 Steel." *Surf. Coat. Technol.*, 2016, 286, 129-139.
9. Riazi, H., Ashrafizadeh, F. and Eslami, A., "Effect of Plasma Nitriding Parameters on Corrosion Performance of 17-4 PH Stainless Steel." *Can. Metall. Q.*, 2017, 56, 322-331.
10. Pessin, M. A., Tier, M. D., Strohaecker, T. R., Bloyce, A., Sun, Y. and Bell, T., "The Effects of Plasma Nitriding Process Parameters on the Wear Characteristics of AISI M2 Tool Steel." *Tribol. lett.*, 2000, 8, 223-228.
11. Wen, D. C., "Plasma Nitriding of Plastic Mold Steel to Increase Wear and Corrosion Properties." *Surf. Coat. Technol.*, 2009, 204, 511-519.
12. Basso, R. L., Pastore, H. O., Schmidt, V., Baumvol, I. J., Abarca, S. A., de Souza, F. S., Spinelli, A., Figueroa, C. A. and Giacomelli, C., "Microstructure and Corrosion Behaviour of Pulsed Plasma-Nitrided AISI H13 Tool Steel." *Corro. Sci.*, 2010, 52, 3133-3139.
13. Nayeypashae, N., Vafaenezhad, H., Kheirandish, Sh. and Soltanieh, M., "Experimental and Numerical Study on Plasma Nitriding of AISI P20 Mold Steel." *Int. J. Miner. Metall. Mater.*, 2016, 23, 1065-1075.
14. Berg, M., Budtz-Jørgensen, C. V., Reitz, H., Schweitz, K. O., Chevallier, J., Kringhøj, P. and Böttiger, J., "On Plasma Nitriding of Steels." *Surf. Coat. Technol.*, 2000, 124, 25-31.
15. De Las Heras, E., Ybarra, G., Lamas, D., Cabo, A., Dalibon, E. L. and Brühl, S. P., "Plasma Nitriding of 316L Stainless Steel in Two Different N<sub>2</sub>-H<sub>2</sub> Atmospheres-Influence on Microstructure and Corrosion Resistance". *Surf. Coat. Technol.*, 2017, 313, 47-54.
16. Das, K., Joseph, A., Ghosh, M. and Mukherjee, S., "Microstructure and Wear Behaviour of Pulsed Plasma Nitrided AISI H13 Tool Steel". *Can. Metall. Q.*, 2016, 55, 402-408.
17. Fenili, C. P., de Souza, F. S., Marin, G., Probst, S. M. H., Binder, C. and Klein, A. N., "Corrosion Resistance of Low-Carbon Steel Modified by Plasma Nitriding and Diamond-like Carbon". *Diam. Relat. Mater.*, 2017, 80, 153-161.
18. Castro, G., Fernandez- Vicente, A. and Cid, J., "Influence of the Nitriding Time in the Wear Behavior of an AISI H13 Steel During a Crankshaft Forging Process". *Wear*, 2007, 263, 1375-1385.
19. Karamis, M. B., "An Investigation of the Properties and Wear Behavior of Plasma-Nitrided Hot-Working Steel (H13) ". *Wear*, 1991, 150, 331-342.
20. Akhtar, S.S., Arif, A.F.M. and Yilbas, B.S., "Influence of Multiple Nitriding on the Case Hardening of H13 Tool Steel: Experimental and Numerical Investigation". *Inter. J. Adv. Manuf. Technol.*, 2012, 58, 57-70.
21. Corengia, P., Ybarra, G., Moína, C., Cabo, A. and Broitman, E., "Microstructural and Topographical Studies of DC-Pulsed Plasma Nitrided AISI 4140 Low-Alloy Steel". *Surf. Coat. Technol.*, 2005, 200, 2391-2397.
22. Forati Rad, H., Amadeh, A. and Moradi, H., "Wear Assessment of Plasma Nitrided AISI H11 Steel". *Mater. Des.*, 2011, 32, 2635-2643.
23. Mohammadzadeh, R., Akbari, A. and Drouet, M., "Microstructure and Wear Properties of AISI M2 Tool Steel on RF Plasma Nitriding at Different N<sub>2</sub>-H<sub>2</sub> Gas Compositions". *Surf. Coat. Technol.*, 2014, 258, 566-573.
24. Mittemeijer, E. J. and Somers, M. A., "Thermodynamics, Kinetics, and Process Control of Nitriding". *Surf. Eng.*, 1997, 13, 483-497.

25. Karamiş, M. B. and Gerçekcioğlu, E., "Wear Behaviour of Plasma Nitrided Steels at Ambient and Elevated Temperatures". *Wear*, 2000, 243, 76-84.
26. Das, K., Alphonsa, J., Ghosh, M., Ghanshyam, J., Rane, R. and Mukherjee, S., "Influence of Pretreatment on Surface Behavior of Duplex Plasma Treated AISI H13 Tool Steel". *Surf. Inter.*, 2017, 206-13.
27. Paschke, H., Weber, M., Braeuer, G., Yilkiran, T., Behrens, B. A. and Brand, H., "Optimized Plasma Nitriding Processes for Efficient Wear Reduction of Forging Dies". *Arch. Civ. Mech. Eng.*, 2012, 12, 407-412.
28. Maniee, A., Mahboubi, F. and Soleimani, R., "The Study of Tribological and Corrosion Behavior of Plasma Nitrided 34CrNiMo6 Steel Under Hot and Cold Wall Conditions". *Mater. Des.*, 2014, 60, 599-604.
29. Mashreghi, A. R., Soleimani, S. M. Y. and Saberifar, S., "The Investigation of Wear and Corrosion behavior of Plasma Nitrided DIN 1.2210 Cold Work Tool Steel". *Mater. Des.*, 2013, 46, 532-538.
30. Wei, M. X., Wang, S. Q., Wang, L., Cui, X. H. and Chen, K. M., "Effect of Tempering Conditions on Wear Resistance in Various Wear Mechanisms of H13 Steel". *Tribol. Inter.*, 2011, 44, 898-905.
31. Saklakoglu, N., "Characterization of Surface Mechanical Properties of H13 Steel Implanted by Plasma Immersion Ion Implantation". *J. Mater. Proc. Technol.*, 2007, 189, 367-73.
32. Aydin, Z., Aldic, G. and Cimenoglu, H., "An Investigation on the Mechanical Properties of the Hard Chromium Layer Deposited by Brush Plating Process on AISI H13 Steel". *Arch. Mater. Sci. Eng.*, 2014, 65, 87-92.
33. Alsaran, A., Altun, H., Karakan, M. and Celik, A., "Effect of Post-Oxidizing on Tribological and Corrosion Behaviour of Plasma Nitrided AISI 5140 Steel". *Surf. Coat. Technol.*, 2004, 176, 344-348.